IEEE Access
Multidisciplinary ⋮ Rapid Review ⋮ Open Access Journal

Received 24 May 2023, accepted 20 June 2023, date of publication 22 June 2023, date of current version 6 July 2023.

Digital Object Identifier 10.1109/ACCESS.2023.3288814

RESEARCH ARTICLE

Chaotic Jaya Optimization Algorithm With Computer Vision-Based Soil Type Classification for Smart Farming

HUSSAIN ALSHAHRANI[1], HEND KHALID ALKAHTANI[2], KHALID MAHMOOD[3], MOFADAL ALYMANI[4], (Member, IEEE), GOUSE PASHA MOHAMMED[5], AMGAD ATTA ABDELMAGEED[5], SITELBANAT ABDELBAGI[5], AND SUHANDA DRAR[5]

[1]Department of Computer Science, College of Computing and Information Technology, Shaqra University, Shaqra 11911, Saudi Arabia
[2]Department of Information Systems, College of Computer and Information Sciences, Princess Nourah bint Abdulrahman University, Riyadh 11671, Saudi Arabia
[3]Department of Information Systems, College of Science and Art at Mahayil, King Khalid University, Abha 61421, Saudi Arabia
[4]Department of Computer Engineering, College of Computing and Information Technology, Shaqra University, Shaqra 11911, Saudi Arabia
[5]Department of Computer and Self Development, Preparatory Year Deanship, Prince Sattam bin Abdulaziz University, Al-Kharj 16273, Saudi Arabia

Corresponding author: Gouse Pasha Mohammed (g.mohammed@psau.edu.sa)

The authors extend their appreciation to the Deanship of Scientific Research at King Khalid University for funding this work through Large Groups Project under grant number (RGP2/112/44). Princess Nourah bint Abdulrahman University Researchers Supporting Project number (PNURSP2023R384), Princess Nourah bint Abdulrahman University, Riyadh, Saudi Arabia. This study is supported via funding from Prince Sattam bin Abdulaziz University project number (PSAU/2023/R/1444).

ABSTRACT Smart farming helps to increase yield by smartly deciding the steps that should be practised in the season. A few components of precision farming are recommending the crops for cultivation, predicting the weather conditions, examining the soil; determining the pesticides, and fertilizers that have to be used. Smart Farming utilizes advanced technologies namely data mining (DM), machine learning (ML), the Internet of Things (IoT), and data analytics for collecting the data, predicting the outcomes and training the system. One of the most significant parameters is proper soil prediction which decides the proper crop and is manually executed by the agriculturalists. Hence, the farmer's efficacy can be improved by producing automated tools for soil type classification. This study presents a Chaotic Jaya Optimization Algorithm with Computer Vision based Soil Type Classification (CJOCV-STC) for smart farming. The presented CJOCV-STC technique applies CV with metaheuristic algorithms for the automated soil classification process, which identifies the soil into distinct types. To accomplish this, the presented CJOCV-STC technique uses the SqueezeNet model for producing a set of feature vectors. To improve the performance of the SqueezeNet model, the CJO algorithm is used for the hyperparameter tuning process. Moreover, the Elman neural network (ENN) technique is applied for soil type classification and the parameters related to it can be adjusted by the chicken swarm algorithm (CSA). The soil classification performance of the CJOCV-STC method can be studied on the Kaggle dataset and the outcomes stated the better performance of the CJOCV-STC algorithm over other recent approaches with increased accuracy of 98.47%.

INDEX TERMS Smart farming, computer vision, soil type classification, deep learning, chaotic systems.

I. INTRODUCTION

Agriculture or farming is the practice of raising cattle and growing crops. It makes a significant contribution to the economy [1]. Several food products and raw materials were produced by agriculture. Raw materials like cotton and jute were utilized by industries to produce several products that are consumed in everyday life [2]. Agriculture not only supports food production but even produces resources required to create commercial products. Traditional farming is typically practised worldwide [3]. Such methods are inaccurate and hence lead to time consumption and hard labour.

The associate editor coordinating the review of this manuscript and approving it for publication was Bo Pu.

The implementation of digital technologies including automation technologies, robots, sensors and electronic devices was linked with Precision Agriculture [4]. This target is to rise profitability, decision management, and reduce work pressures.

Soil becomes a basic element in the nutrient supply and the crop yield to the crops and results in the growth of the redundant weed from soil because of fertility [5]. Soil classification laid the foundation for several fields like land consolidation, crop management, and soil improvement [6]. Physical properties such as temperature and moisture affect pores and particle formation, which affects water infiltration, root growth, and plant emergence speed, finally crop yield [7]. Chemical features like the NPK parameters, pH, and organic carbon determine the mobility of contaminants, obtainability of nutrients, and the incidence of other species.

Machine learning (ML) makes agricultural applications simple and efficient [8]. Generalization, Data acquisition, and model building are the three phases of the ML process. In many cases, ML techniques were utilized to deal with complicated issues when human competence is inadequate. ML may be used in agriculture to predict soil variables like organic carbon and moisture content, crop yield prediction, weed and disease detection in species and crop detection [9]. Deep Learning (DL) improves conventional ML by adding additional complexity to the model and varying the input with different functions that let data representation hierarchically with many levels of abstraction, relying upon the network architecture. The ability to find unknown things like anomalies instead of collecting existing items is a main aspect of the DL method [10], which utilizes the homogeneous properties of an agricultural domain to find unknown, faraway, and badly obstructed objects.

Al-Naji et al. [11] present a non-contact vision system based on the video camera to forecast the irrigation requirement for loam soils by implementing a feedforward BPNN. The presented method utilized this colour data as input to the ANN method for deciding whether to irrigate soil or not. In [12], the authors addressed the soil nutrient analysis by regression procedure and its spectral index related to the forecast procedure through Iterative Self-Organizing (ISO) cluster unsupervised categorizing procedure. Suruliandi et al. [13] focused on the design of an optimal feature selection approach for the crop prediction process. The research outcome demonstrates the Recursive Feature Elimination (RFE) procedure with Adaptive Bagging (AB) categorizer that exceeds other individuals.

In [14], the fundamental parameters were decided by employing a soil map and the Shuttle Radar Topography Mission record. Land use competence classes, erosion hazard, soil depth, and other characteristics are attained from soil map, and elevation, while slop, and factors were attained from Shuttle Radar Topography Mission record. In [15], advanced Adaboost methods are devised to categorize soil kinds based on tree algorithm methods that are less frequently utilized in this field. Srivastava et al. [16] discuss diverse computer-oriented soil categorization practices separated into 2 main streams. The first is CV-related soil categorization and image processing methods which encompasses the traditional image processing procedures and models to categorize soil by implementing diverse factors such as particle size, texture, and colour. Second is ML and DL-based soil categorization approaches like CNN which provide modernized outcomes.

Azadnia et al. [17] suggest a transportable smartphone-related machine vision structure by employing CNN for the categorization of soil texture imagery from 20, 40, and 60 cm heights. The presented CNN approach comprises 2 blocks with many distinct layers. The initial block (extraction feature) comprises batch normalization, Conv, dropout, and Max-pooling layers. The second comprises SVM methods, FC layers, and flattening. During this case, the SVM, ANN, RF, and KNN techniques are utilized for comparing the presented CNN outcomes with other classifiers. The outcomes exposed the presented CNN algorithm can rapidly forecast the kind of soil textures on huge scale farms and so be an optimum substitute to expensive and time-taking lab approaches.

Although many ML and DL algorithms were available in this study for soil classification, still it needed to improve the performance of the classification. Also, the number of parameters of the DL algorithm quickly increases owing to its continuous deepening of the model, resulting in model overfitting. Together, many hyperparameters have a significant effect on the efficacy of the CNN model. Especially, hyperparameters like learning rate selection, batch size, and epoch count are crucial to obtain superior outcomes. In the meantime, the trial and error technique for hyperparameter tuning is a challenging and tedious task, metaheuristic algorithm is used.

This study proposes a Chaotic Jaya Optimization Algorithm with Computer Vision based Soil Type Classification (CJOCV-STC) for smart farming. The presented CJOCV-STC technique uses the SqueezeNet model for producing a set of feature vectors. The CJO algorithm is exploited for the hyperparameter tuning to enhance the performance of the SqueezeNet model. Moreover, the Elman neural network (ENN) technique was applied for the soil type classification and the parameters related to it can be adjusted by the chicken swarm algorithm (CSA). The soil classification performance of the CJOCV-STC method can be studied on the Kaggle dataset.

- An intelligent CJOCV-STC model comprising SqueezeNet feature extraction, CJO-based hyperparameter tuning, ENN classification, and CSA-based parameter tuning is presented. To the best of our knowledge, the proposed CJOCV-STC technique never existed in the literature.
- Employ the CJO algorithm for hyperparameter tuning, which incorporates chaotic dynamics into the JOA to enhance its exploration and exploitation capabilities. By introducing chaos, the algorithm is expected to achieve a better balance between the exploration of the solution space and the exploitation of promising regions.

- Hyperparameter tuning of the SqueezeNet model and ENN model using CJO and CSA helps to improve the soil classification performance on unseen data.

The rest of the paper is organized in the following. Section II provides the proposed model. Later, section III provides the result analysis and section IV concludes the paper.

II. THE PROPOSED MODEL

In this study, a new CJOCV-STC method was proposed for automated soil type classification in the smart farming sector by the use of CV and metaheuristic algorithms. In the presented CJOCV-STC technique, various subprocesses are involved namely SqueezeNet feature vector generation, CJO-based hyperparameter tuning, ENN-based classification, and CSO-based parameter optimization. Fig. 1 illustrates the workflow of the CJOCV-STC approach.

A. FEATURE EXTRACTION: OPTIMAL SQUEEZE NET MODEL

In this work, the SqueezeNet model was used for feature vector generation. The technique for the feature extraction utilizes a SqueezeNet approach which has previously been trained [18]. The SqueezeNet scheme assumes the input image develops forward and works as an extraction feature but still it attains a layer previously set (extraction feature layer). The procedure ends here, having the final layer output. The SqueezeNet approach of pretrained CNN was employed in this presented method. SqueezeNet is a new version of the CNN algorithm that utilizes just 3×3 and 1×1 convolution layers. Here fire module is the kterm indicating constructing block of SqueezeNet.

A fire module contains a convolutional layer with ''expand'' and ''squeeze'' layers. Initially, the input image passes through a convolution layer termed ''conv1''. A squeeze convolution layer has one filter. It is provided as an expanded layer that comprises a combination of 1×1 and 3×3 convolutional filters which capture spatial data (extraction feature) at several scales. This layer has afterwards 8 ''fire modules,'' numbered ''fire2'' through ''fire9''. After fire8, fire4, conv10, and conv1, max-pooling layers have been executed with a stride of 2. Dropout layers can be included in the Fire9 module for reducing over-fitting. Downsampling has been placed late, which leads to SqueezeNet with a ''complex bypass''.

The CJO model is exploited for the hyperparameter tuning to enrich the performance of the SqueezeNet model [19]. The objective of leveraging chaos in an optimizer technique is to use its easier implementation, better dynamic behaviour and exceptional capability to improve the diversity of the population. The study integrated chaos in the JO algorithm to avoid falling in local optima and enhance its searching behaviour.

The logistic map is a higher sensitivity to the slight modification of an initial condition, the random-like and ergodic and also 1D chaotic system can be determined using the subsequent formula:

$$\beta^{k+1} = \mu\beta^k \left(1 - \beta^k\right), k = 1, 2, \ldots \beta \in [0, 1] \quad (1)$$

In Eq. (1), $\in [0, 4)$. The chaotic map can be determined in the interval. The bifurcation diagram of the logistic map is the fruit of plotting, as a function of μ, a sequence of values for β, accomplished by beginning with a random integer, which iterates it several times and eliminates the initial point respective to the value beforehand the iterates converge towards the attractor. The chaotic map is embedded in an optimized technique due to the pseudo-random behaviour. The sensitivity of the initial condition and control parameter enables better outcomes in the generation of chaotic sequences. In the presented method, the logistic map was leveraged for substituting arbitrary numbers in the original JO technique.

The original JO technique suffers from certain shortcomings namely lack of population diversity and premature convergence. As a result, it might fall into local optimal. The efficiency of the presented technique is primarily related to accomplishing a compromise between exploration and exploitation capabilities. The exploitation is connected to the convergence towards the optimum solution in a speedy way. On the other hand, exploration can be recognized as the examination of the potential area in the search space.

The authors recommended the new CJO algorithm by incorporating chaos in the typical JO algorithm. The three mutually exclusive search expressions are proposed to obtain a compromise between exploitation and exploration, as defined in Eqs. (2)-(4):

$$X_{new,j} = C_{i,j}Xrand_{i,j} + C_{i,j}(X_{i,j} - C_{i,j}Xrand_{i,j}) + C_{i,j}\left(X_{bestj} - C_{i,j}Xrand_{i,j}\right) \quad (2)$$

$$X_{new,j} = C_{i,j}Xrand_{i,j} + C_{i,j}\left(X_{i,j} - C_{i,j}Xrand_{i,j}\right) + C_{i,j}\left(X_{worst,j} - C_{i,j}Xrand_{i,j}\right) \quad (3)$$

$$X_{new,j} = C_{i,j}Xbest_j + C_{i,j}\left(Xrand_{i,j} - S_F Xbest_j\right) \quad (4)$$

where $C_{i,j}$ indicates the values of chaotic numbers generated using the logistic map. The variable S_F could chaotically take two values (1 or 2). The local search capability of the CJO algorithm can be enhanced by Eq. (4). Early convergence can be commonly encountered due to a massive amount of local optimal. Thus, the global optima could not be attained. These problems are tackled while the scaling factor has taken its maximal value. In such cases, trapping in local optimal was prevented, and search behaviours can be improved.

B. SOIL TYPE CLASSIFICATION: ENN MODEL

The ENN method was exploited in this study for the identification and classification of soil into diverse types. The four main layers involved in the ENN model are the input layer, a hidden layer (HL), an output layer, and a context layer [20]. The basic configuration of this NN is like feedforward NN so that the connection in the HL, output, and input layers is exactly alike the multi-layer NN. In addition, the context layer

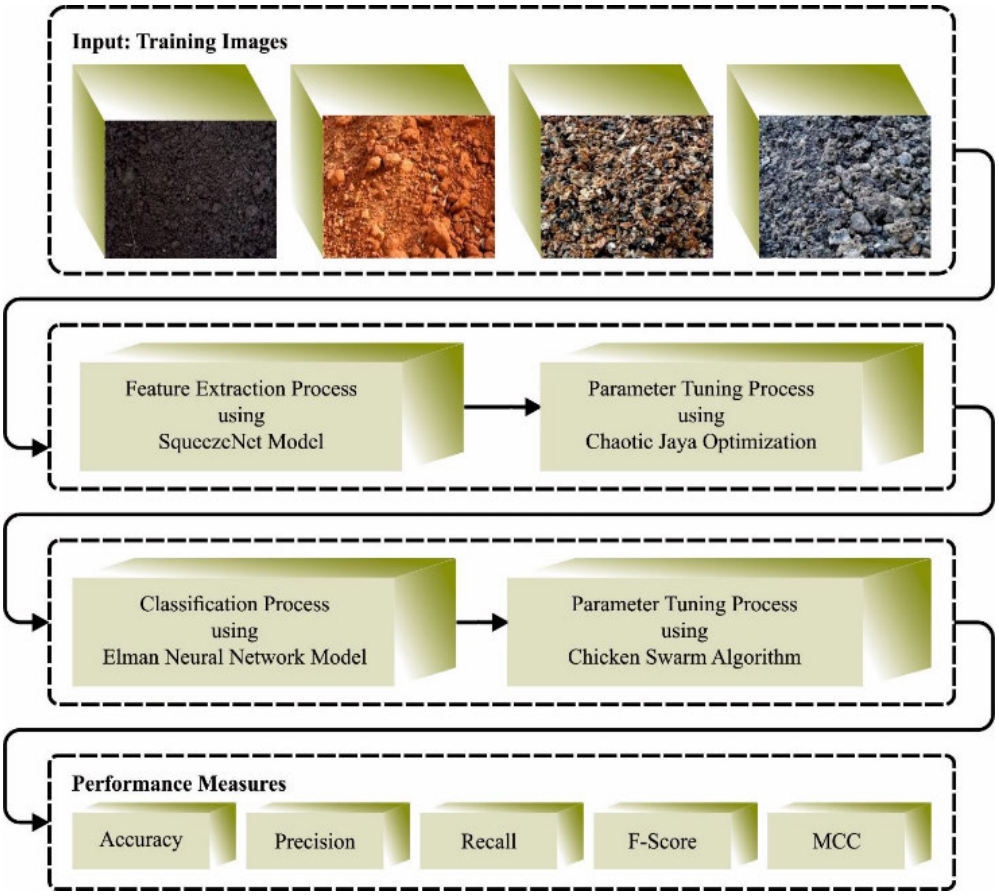

FIGURE 1. Working flow of CJOCV-STC approach.

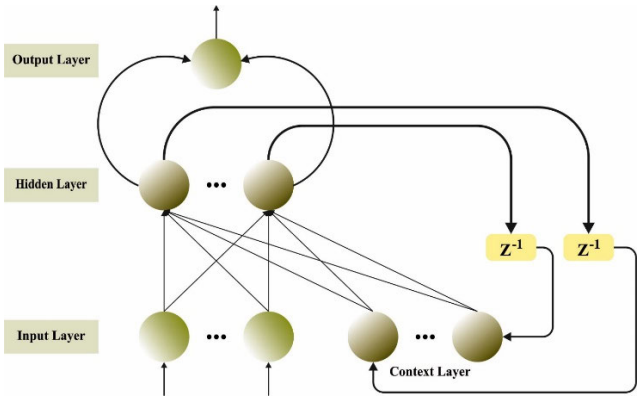

FIGURE 2. The architecture of the ENN model.

was another layer in ENN that existed so that the input derived from the output of the HL is used to store the prior value of the HL.

Fig. 2 illustrates the structure of ENN. The WV_h^i, WV_h^c, and WV_h^0 correspondingly the output weight matrices, external input, and context weight. Concerning the form of ENN, the dimension of the output and input layers were n and the dimension of the context layer is m, viz., $x^1(t) = [x_1^1(t), x_2^1(t), \ldots, x_n^1(t)]^T$ and $y(t) = [y_1(t), y_2(t), \ldots, y_n(t)]^T$. In this network, the input layer is modelled as follows:

$$u_i(l) = e_i(l), i = 1, 2, \ldots, n \tag{5}$$

In Eq. (5), l demonstrates the input and the output layer at the $l - th$ iteration and the $k - th$ HLs can be formulated by:

$$v_k(l) = \sum_{j=1}^{N} \omega_{kj}^1(l)\, x_j^c(l) + \sum_{i=1}^{N} \omega_{ki}^2(l)\, u_i(l), k = 1, 2, \ldots, N \tag{6}$$

In Eq. (6), $x_j^c(l)$ defines the forwarded signal from the kth context layer nodes, $and \omega_{kj}^1(l)$ determines the i^{th} and j^{th} weights of HLs transmitted from the oth node. Thus, the weight of $k - th$ HL was accomplished using $\omega_{ki}^2(l)$ for the input layer. Lastly, the output values of HL which are added to the context layer can be attained by Eq. (7):

$$W_k(l) = f_0(\bar{v}_k(l)) \tag{7}$$

where

$$\bar{v}(l) = \frac{v_k(l)}{\max\{v_k(l)\}} \tag{8}$$

Eq. (7) is the normalized value of the HL and Eq. (8) is the context layer. Now, the output is equal to the Eq. (9):

$$C_k(l) = \beta_k(l-1) + WV_k(l-1), k = 1, 2, \ldots, N \quad (9)$$

In Eq. (9), WV_k refers to the gain of self-connected feedback between [0, 1]. Lastly, the output layer can be represented as follows:

$$y_0(l) = \sum_{k=1}^{N} \omega_{0/e}^{3}(l)\, WV_k(l)\, 0 = 1, 2, \ldots, n \quad (10)$$

In Eq. (10), $\omega_{0/e}^{3}$ determines the weight connection from k^{th} into o^{th} layers.

C. HYPERPARAMETER TUNING: CSA

Finally, the CSA is utilized for the optimal parameter adjustment of the ENN algorithm. The CSA inspires hierarchal order from CS and the performance of CS which stems from the performance of bird foraging actions [21]. The CS has been categorized into several groups such as one rooster, several hens, and many chicks. Roosters continuously explore for optimal food in the foraging. The hens frequently track the rooster for finding food, and the chicks track their mother to find food. An individual surrounded by CS complies with different laws of motion. There would be competition amongst individuals with CS in a particular hierarchal order. The place of each individual with CS portrays a feasible result of the optimizer system. Primarily, define the variable beforehand determining the position upgrade formula of individuals within the CS: H_N, R_N, M_N, and $C_N$correspondingly demonstrates the hen, rooster, mother hen, and chick counts; N implies the count of CSs, D signifies the dimensional of problems; $x_{i,j}(t)(i \in [1, \cdots, N], j \in [1, \cdots, D])$ denotes a place of individuality time t.

During the CS, the best R_N chicken can be regraded rooster, but the worse C_N one was observed as a chick. The remaining CS was viewed as a hen. Rooster having best fitting values takes a major problem for food accessing if related to one with worst fitting value and it can be expressed in the Eqs. (11)-(12):

$$x_{i,j}(t+1) = x_{i,j}(t)\left(1 + Randn\left(0, \sigma^2\right)\right) \quad (11)$$

$$\sigma^2 = \begin{cases} 1, & f_i \geq f_k, k \in [1, N], k \neq i \\ exp\left(\dfrac{f_k - f_i}{|f_i| + \varepsilon}\right), & otherwise, \end{cases} \quad (12)$$

In Eq. (12), Randn $(0, \sigma^2)$ stands for Gaussian distribution taking standard deviation σ and mean $0, \varepsilon$ displays the least constant to avoid zero-division-error, k shows the rooster index, which is haphazardly selected in the rooster groups, $(k \neq i), f_i$ refers fitness value of particles i.

Intended for the hens, it follows a group-mate rooster for finding food and randomly takes food found by others as given in Eqs. (13)-(15):

$$X_{i,j}^{t+1} = X_{i,j}^{t} + C_1 Rand(X_{r1,j}^{t} - X_{i,j}^{t}) + C_2 Rand(X_{r2,j}^{t} - X_{i,j}^{t}) \quad (13)$$

$$C_1 = \exp((f_i - f_{r1})/(|f_i| + \varepsilon \quad (14)$$

$$C_2 = \exp((f_{r2} - f_i)) \quad (15)$$

where *Rand* shows uniformly distributed random integer in $[0, 1], r_1$ implies the index of roosters, viz i^{th} hen's groupmate, and r_2 signifies the index of chickens which is selected randomly in the CS $r_1 \neq r_2$.Concerning the chicks, it is following their mother for foraging for food and it can be demonstrated in Eq. (16):

$$X_{i,j}^{t+1} = X_{i,j}^{t} + F\left(X_{m,j}^{t} - X_{i,j}^{t}\right) \quad (16)$$

But $x_{m,j}(t)$ signifies the place of the chick's mother, $F \in [0, 2]$ followed by co-efficient signifies that the chick tracks its mother for foraging for food. The CSA approach has derived a fitness function to get optimal performance of the classification. It ascertains a positive value to denote the superior outcome of the solution candidate. Herein, the decline of the classifier error rate was the fitness function, as seen in Eq. (17).

$$fitness(x_i) = \frac{number\ of\ misclassified\ samples}{Total\ number\ of\ samples} * 100 \quad (17)$$

III. RESULTS AND DISCUSSION

The proposed method is simulated utilizing Python 3.6.5 tool on PC i5-8600k, 250GB SSD, GeForce 1050Ti 4GB, 1TB HDD, and 16 GB RAM. The parameter settings are represented in the following: epoch counts 50, batch size: 5, learning rate: 0.01, dropout: 0.5, and activation: ReLU. The Python packages utilized are Keras, TensorFlow (GPU-CUDA Enabled), numpy, pickle, sklearn, pillow, matplotlib, and opencv-python.

In this study, the soil type recognition performance of the CJOCV-STC technique can be studied on the dataset [22], containing 280 samples with seven classes. The details related to this dataset are described in Table 1. Fig. 3 characterizes the sample images.

TABLE 1. Details of the dataset.

Class	No. of Instances
Clayey Sand (CS)	40
Sandy Clay (SC)	40
Silty Sand (SS)	40
Clay (Clay)	40
Humus Clay (HC)	40
Clayey Peat (CP)	40
Peat (Peat)	40
Total No. of Instances	280

The sand type recognition output of the CJOCV-STC technique is demonstrated in Fig. 4 in the way of a confusion

FIGURE 3. Sample soil-type images.

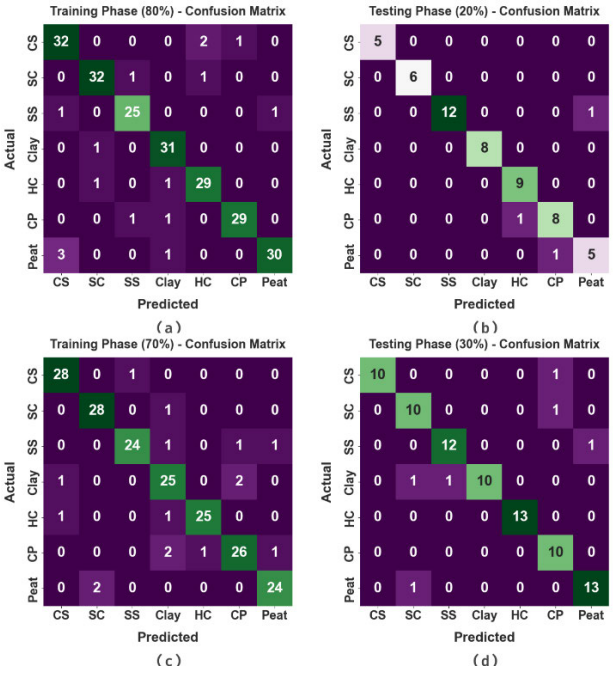

FIGURE 4. Confusion matrices of CJOCV-STC algorithm (a-b) 80:20 of TRP/TSP and (c-d) 70:30 of TRP/TSP.

matrix. The figure identifies that the CJOCV-STC technique proficiently identified and categorized various kinds of sands with 80:20 and 70:30 of TRP/TSP.

In Table 2 and Fig. 5, the entire sand classification outcomes of the CJOCV-STC technique are studied well. The table values notify the improvised performance of the CJOCV-STC technique under 80:20 of TRP/TSP. With 70% of TRP, the CJOCV-STC technique attains an average $accu_y$ of 97.96%, $prec_n$ of 92.98%, $reca_l$ of 92.91%, F_{score} of 92.89%, and MCC of 91.73%. Besides, with 30% of TSP, the CJOCV-STC approach attains an average $accu_y$ of 98.47%, $prec_n$ of 94.60%, $reca_l$ of 94.93%, F_{score} of 94.71%, and MCC of 93.85%.

TABLE 2. Sand classifier outcome of CJOCV-STC approach under 80:20 of TRP/TSP.

Class	$Accu_y$	$Prec_n$	$Reca_l$	F_{score}	MCC
Training Phase (80%)					
CS	96.88	88.89	91.43	90.14	88.30
SC	98.21	94.12	94.12	94.12	93.07
SS	98.21	92.59	92.59	92.59	91.58
Clay	98.21	91.18	96.88	93.94	92.95
HC	97.77	90.62	93.55	92.06	90.78
CP	98.66	96.67	93.55	95.08	94.32
Peat	97.77	96.77	88.24	92.31	91.14
Average	97.96	92.98	92.91	92.89	91.73
Testing Phase (20%)					
CS	100.00	100.00	100.00	100.00	100.00
SC	100.00	100.00	100.00	100.00	100.00
SS	98.21	100.00	92.31	96.00	94.98
Clay	100.00	100.00	100.00	100.00	100.00
HC	98.21	90.00	100.00	94.74	93.85
CP	96.43	88.89	88.89	88.89	86.76
Peat	96.43	83.33	83.33	83.33	81.33
Average	98.47	94.60	94.93	94.71	93.85

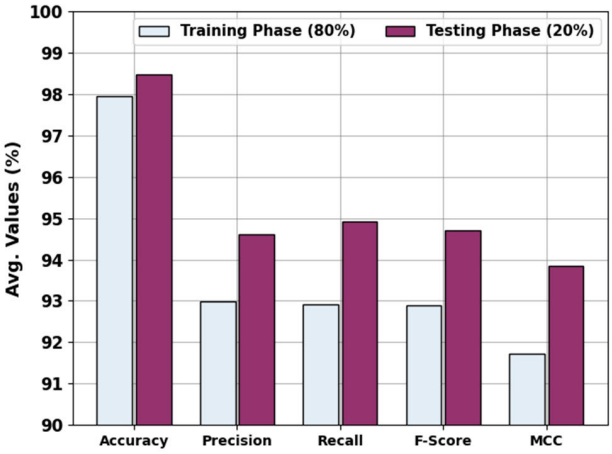

FIGURE 5. Average soil classification results of CJOCV-STC approach under 80:20 of TRP/TSP.

In Table 3 and Fig. 6, the entire sand classification outcomes of the CJOCV-STC method are studied well. The table values notify the improvised performance of the CJOCV-STC approach under 70:30 of TRP/TSP. With 70% of TRP, the CJOCV-STC method attains an average $accu_y$ of 97.67%, $prec_n$ of 92.02%, $reca_l$ of 91.84%, F_{score} of 91.88%, and MCC of 90.55%. Besides, with 30% of TSP, the CJOCV-STC algorithm attains an average $accu_y$ of 97.96%, $prec_n$ of 93.12%, $reca_l$ of 92.90%, F_{score} of 92.74%, and MCC of 91.73%.

Fig. 7 inspects the accuracy of the CJOCV-STC technique during the training and validation process on the test dataset. The figure notifies that the CJOCV-STC method reaches

TABLE 3. Sand classifier outcome of CJOCV-STC method under 70:30 of TRP/TSP.

Class	$Accu_y$	$Prec_n$	$Reca_l$	F_{score}	MCC
Training Phase (70%)					
CS	98.47	93.33	96.55	94.92	94.03
SC	98.47	93.33	96.55	94.92	94.03
SS	97.96	96.00	88.89	92.31	91.22
Clay	95.92	83.33	89.29	86.21	83.88
HC	98.47	96.15	92.59	94.34	93.48
CP	96.43	89.66	86.67	88.14	86.05
Peat	97.96	92.31	92.31	92.31	91.13
Average	97.67	92.02	91.84	91.88	90.55
Testing Phase (30%)					
CS	98.81	100.00	90.91	95.24	94.70
SC	96.43	83.33	90.91	86.96	85.00
SS	97.62	92.31	92.31	92.31	90.90
Clay	97.62	100.00	83.33	90.91	90.05
HC	100.00	100.00	100.00	100.00	100.00
CP	97.62	83.33	100.00	90.91	90.05
Peat	97.62	92.86	92.86	92.86	91.43
Average	97.96	93.12	92.90	92.74	91.73

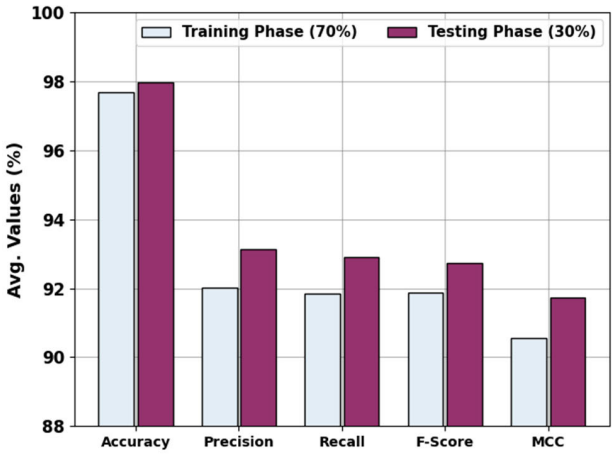

FIGURE 6. Average soil classification results of CJOCV-STC approach under 70:30 of TRP/TSP.

increasing accuracy values over increasing epochs. As well, the increasing validation accuracy over training accuracy shows that the CJOCV-STC technique learns efficiently on the test dataset.

The loss analysis of the CJOCV-STC technique at the time of training and validation is given on the test dataset in Fig. 8. The outcomes indicate that the CJOCV-STC method reaches closer values of training and validation loss. The CJOCV-STC technique learns efficiently on the test dataset.

A brief precision-recall (PR) curve of the CJOCV-STC method is demonstrated on the test dataset in Fig. 9. The outcomes stated that the CJOCV-STC technique results in

FIGURE 7. Training and validation accuracy curves of the CJOCV-STC approach.

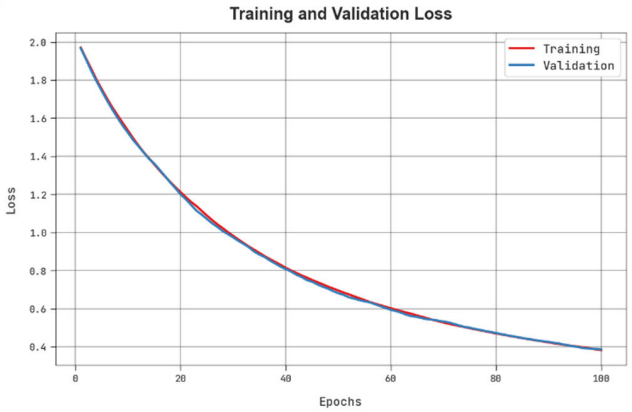

FIGURE 8. Training and validation loss curves of the CJOCV-STC approach.

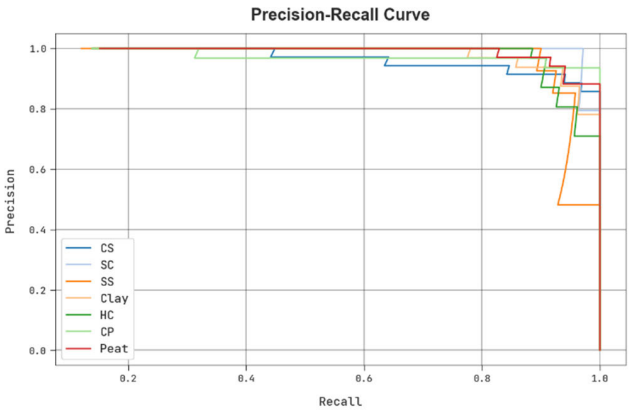

FIGURE 9. The precision-recall curve of the CJOCV-STC approach.

increasing values of PR. Additionally, the CJOCV-STC technique can reach higher PR values in all classes.

In Fig. 10, a ROC study of the CJOCV-STC method is revealed on the test dataset. The figure described that the CJOCV-STC method resulted in improved ROC values. Besides, the CJOCV-STC technique can extend enhanced ROC values in all classes.

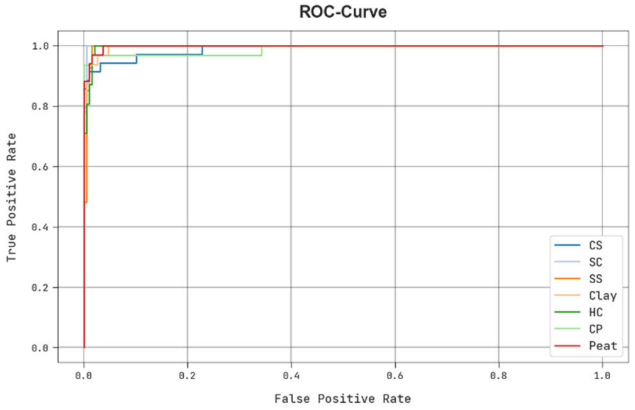

FIGURE 10. ROC curve of the CJOCV-STC approach.

TABLE 4. Comparative outcome of CJOCV-STC method with other systems [23].

Methods	$Accu_y$	$Prec_n$	$Reca_l$	F_{score}
CJOCV-STC	98.47	94.60	94.93	94.71
PSO model	77.60	77.47	77.48	77.57
GSA model	77.58	79.04	78.06	78.96
DE model	78.00	78.30	78.00	78.21
SMO model	78.19	78.84	78.39	78.93
CSMO model	82.15	80.85	80.56	82.24
FCMCSO-ASC	89.86	89.84	92.72	90.32

To highlight the improvements of the CJOCV-STC system, a widespread comparison study is performed in Table 4 [23]. In Fig. 11, a comparative $accu_y$ and F_{score} assessment of the CJOCV-STC technique with existing models. The results demonstrate that the CJOCV-STC technique results in improved values of $accu_y$ and F_{score} of 98.47% and 94.71%. At the same time, the PSO, GSA, DE, and SMO models showcase lower classifier results. Although the CSMO and FCMCSO-ASC models accomplish considerable outcomes, they failed to outperform the CJOCV-STC technique.

In Fig. 12, the detailed $prec_n$ and $reca_l$ assessment of the CJOCV-STC method with existing models. The outcomes exhibit that the CJOCV-STC method that has superior values of $prec_n$ and $reca_l$ of 94.60% and 94.93%. Simultaneously, the PSO, GSA, DE, and SMO approaches display lower classifier results.

Although the CSMO and FCMCSO-ASC methods accomplish considerable outcomes, they failed to outperform the CJOCV-STC algorithm. These results highlighted the enhanced performance of the CJOCV-STC method on the soil type classification process. The enhanced performance of the proposed model is due to the inclusion of a hyperparameter tuning process. In addition, the CJO algorithm integrates chaotic concepts to achieve a better balance between the exploration of the solution space and the exploitation of promising regions. The CJO and CSO algorithms choose the

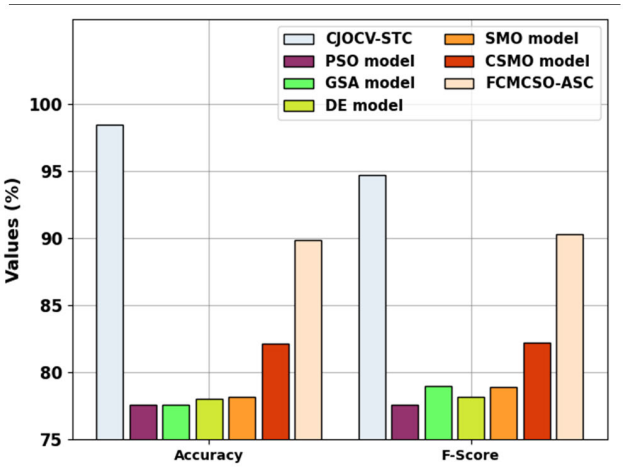

FIGURE 11. $Accu_y$ and F_{score} outcome of CJOCV-STC algorithm with soil type classifiers.

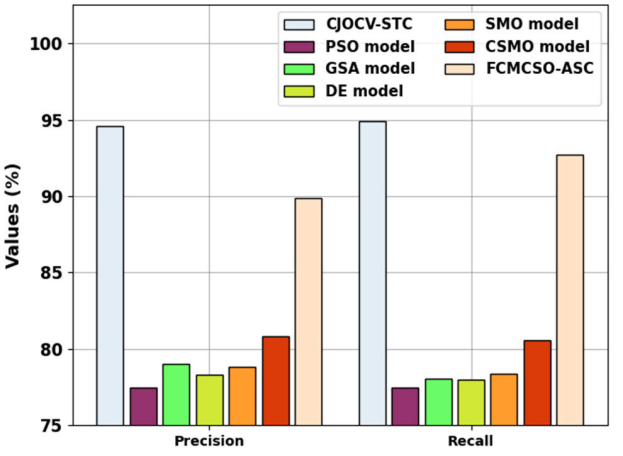

FIGURE 12. $Prec_n$ and $Reca_l$ outcome of CJOCV-STC algorithm with soil type classifiers.

optimal values for the hyperparameters of the SqueezeNet and ENN models respectively. They can have a significant impact on the performance of the model, and selecting the optimal values can lead to better accuracy. By combining CJO and CSO-based hyperparameter tuning, the proposed model can achieve even better results by focusing on selecting the optimal settings for the algorithm. These results ensured the improved performance of the proposed technique over other existing techniques.

IV. CONCLUSION

In this study, a new CJOCV-STC method was proposed for automated soil type classification in the smart farming sector by the use of CV and metaheuristic algorithms. In the presented CJOCV-STC technique, various subprocesses are involved namely SqueezeNet feature vector generation, CJO-based hyperparameter tuning, ENN-based classification, and CSO-based parameter optimization. The CJO approach is

used for the hyperparameter tuning process to enhance the performance of the SqueezeNet method. Furthermore, the CSA with ENN model is exploited for the recognition and classification of soil into diverse types. The soil classification performance of the CJOCV-STC method can be studied on the Kaggle dataset and the outcomes demonstrated better performance of the CJOCV-STC algorithm over other existing techniques with 98.47% of maximum accuracy. In the upcoming years, the presented CJOCV-STC technique can be extended to the soil type classification on remote sensing images. In addition, the proposed model can be tested on a large-scale real-time dataset, comprising region-wise distinct soil types.

ACKNOWLEDGMENT

The authors extend their appreciation to the Deanship of Scientific Research at King Khalid University for funding this work through Large Groups Project under grant number (RGP2/112/44). Princess Nourah bint Abdulrahman University Researchers Supporting Project number (PNURSP2023R384), Princess Nourah bint Abdulrahman University, Riyadh, Saudi Arabia. This study is supported via funding from Prince Sattam bin Abdulaziz University project number (PSAU/2023/R/1444).

REFERENCES

[1] H. Mugiyo, V. G. P. Chimonyo, M. Sibanda, R. Kunz, C. R. Masemola, A. T. Modi, and T. Mabhaudhi, "Evaluation of land suitability methods with reference to neglected and underutilised crop species: A scoping review," *Land*, vol. 10, no. 2, p. 125, Jan. 2021.

[2] L. Ding, X. Wang, Z. Ouyang, Y. Chen, X. Wang, D. Liu, S. Liu, X. Yang, H. Jia, and X. Guo, "The occurrence of microplastic in Mu Us and land soils in northwest China: Different soil types, vegetation cover and restoration years," *J. Hazardous Mater.*, vol. 403, Feb. 2021, Art. no. 123982.

[3] B. Kashyap and R. Kumar, "Sensing methodologies in agriculture for soil moisture and nutrient monitoring," *IEEE Access*, vol. 9, pp. 14095–14121, 2021.

[4] P. Taneja, H. K. Vasava, P. Daggupati, and A. Biswas, "Multi-algorithm comparison to predict soil organic matter and soil moisture content from cell phone images," *Geoderma*, vol. 385, Mar. 2021, Art. no. 114863.

[5] S. M. Pande, P. K. Ramesh, A. Anmol, B. R. Aishwarya, K. Rohilla, and K. Shaurya, "Crop recommender system using machine learning approach," in *Proc. 5th Int. Conf. Comput. Methodologies Commun. (ICCMC)*, Apr. 2021, pp. 1066–1071.

[6] V. Habibi, H. Ahmadi, M. Jafari, and A. Moeini, "Mapping soil salinity using a combined spectral and topographical indices with artificial neural network," *PLoS ONE*, vol. 16, no. 5, May 2021, Art. no. e0228494.

[7] C. Luo, Y. Wang, X. Zhang, W. Zhang, and H. Liu, "Spatial prediction of soil organic matter content using multiyear synthetic images and partitioning algorithms," *CATENA*, vol. 211, Apr. 2022, Art. no. 106023.

[8] K. Nabiollahi, R. Taghizadeh-Mehrjardi, A. Shahabi, B. Heung, A. Amirian-Chakan, M. Davari, and T. Scholten, "Assessing agricultural salt-affected land using digital soil mapping and hybridized random forests," *Geoderma*, vol. 385, Mar. 2021, Art. no. 114858.

[9] A. Jagetia, U. Goenka, P. Kumari, and M. Samuel, "Visual transformer for soil classification," in *Proc. IEEE Students Conf. Eng. Syst. (SCES)*, Jul. 2022, pp. 1–6.

[10] X. Li, P. Fan, Z. Li, G. Chen, H. Qiu, and G. Hou, "Soil classification based on deep learning algorithm and visible near-infrared spectroscopy," *J. Spectrosc.*, vol. 2021, pp. 1–11, Sep. 2021.

[11] A. Al-Naji, A. B. Fakhri, S. K. Gharghan, and J. Chahl, "Soil color analysis based on a RGB camera and an artificial neural network towards smart irrigation: A pilot study," *Heliyon*, vol. 7, no. 1, Jan. 2021, Art. no. e06078.

[12] V. A. Gulhane, S. V. Rode, and C. B. Pande, "Correlation analysis of soil nutrients and prediction model through ISO cluster unsupervised classification with multispectral data," *Multimedia Tools Appl.*, vol. 82, no. 2, pp. 2165–2184, Jan. 2023.

[13] A. Suruliandi, G. Mariammal, and S. P. Raja, "Crop prediction based on soil and environmental characteristics using feature selection techniques," *Math. Comput. Model. Dyn. Syst.*, vol. 27, no. 1, pp. 117–140, Jan. 2021.

[14] T. Everest, A. Sungur, and H. Özcan, "Determination of agricultural land suitability with a multiple-criteria decision-making method in northwestern Turkey," *Int. J. Environ. Sci. Technol.*, vol. 18, no. 5, pp. 1073–1088, May 2021.

[15] B. T. Pham, M. D. Nguyen, T. Nguyen-Thoi, L. S. Ho, M. Koopialipoor, N. K. Quoc, D. J. Armaghani, and H. V. Le, "A novel approach for classification of soils based on laboratory tests using AdaBoost, tree and ANN modeling," *Transp. Geotechnics*, vol. 27, Mar. 2021, Art. no. 100508.

[16] P. Srivastava, A. Shukla, and A. Bansal, "A comprehensive review on soil classification using deep learning and computer vision techniques," *Multimedia Tools Appl.*, vol. 80, no. 10, pp. 14887–14914, Apr. 2021.

[17] R. Azadnia, A. Jahanbakhshi, S. Rashidi, M. Khajehzadeh, and P. Bazyar, "Developing an automated monitoring system for fast and accurate prediction of soil texture using an image-based deep learning network and machine vision system," *Measurement*, vol. 190, Feb. 2022, Art. no. 110669.

[18] G. Ciaburro, S. Padmanabhan, Y. Maleh, and V. Puyana-Romero, "Fan fault diagnosis using acoustic emission and deep learning methods," *Informatics*, vol. 10, no. 1, p. 24, Feb. 2023.

[19] B. M. Alshammari, A. Farah, K. Alqunun, and T. Guesmi, "Robust design of dual-input power system stabilizer using chaotic Jaya algorithm," *Energies*, vol. 14, no. 17, p. 5294, Aug. 2021.

[20] D. Yu, Y. Wang, H. Liu, K. Jermsittiparsert, and N. Razmjooy, "System identification of PEM fuel cells using an improved Elman neural network and a new hybrid optimization algorithm," *Energy Rep.*, vol. 5, pp. 1365–1374, Nov. 2019.

[21] Y. Yu, M. Rashidi, B. Samali, M. Mohammadi, T. N. Nguyen, and X. Zhou, "Crack detection of concrete structures using deep convolutional neural networks optimized by enhanced chicken swarm algorithm," *Struct. Health Monitor.*, vol. 21, no. 5, pp. 2244–2263, Sep. 2022.

[22] B. Bhattacharya and D. P. Solomatine, "Machine learning in soil classification," *Neural Netw.*, vol. 19, no. 2, pp. 186–195, Mar. 2006.

[23] A. K. Dutta, Y. Albagory, M. A. Faraj, M. Alsanea, and A. R. W. Sait, "Cat swarm with fuzzy cognitive maps for automated soil classification," *Comput. Syst. Sci. Eng.*, vol. 44, no. 2, pp. 1419–1432, 2023.